Fuzzy Control of Laparoscopic Surgical Robot Designed for Use in Minimally Invasive Surgery

Serhat Aksungur[1], Oğuz Yakut*[2]

Abstract: Nowadays, the use of robot technologies has become widespread. Robots that have been confronted in many sectors have also been used in surgical operations in recent years. RCM (Remote Center of Motion) mechanisms take the place of these robots, which have less space-consuming and specially designed for operation. Reduced space requirements and lower maintenance costs are the greatest advantages of these mechanisms.

In this study, some of the RCM mechanisms which used in surgical operations are mentioned. A unique and original surgical robot designed for laparoscopic surgical purposes which is not in the literature of robots, has been described. This surgical robot was designed with a 3D CAD program and motion of robot was analyzed. Robot control was performed using fuzzy control method. Dynamic equations of robot which used at fuzzy control were obtained with Lagrangian mechanics. MATLAB software has been used for robot control. Used membership function parameters of fuzzy control were optimized with genetic algorithm method. Obtained fuzzy control graphics with MATLAB were given in the result section.

Keywords: Surgical robot, RCM mechanism, Lagrangian motion equations, fuzzy control

1. Introduction

Nowadays, surgical applications, entering the body through a small incision with laparoscopic procedures are performed and are expanding the use of robots for these operations. In existing systems, conventional robots are used as body of surgical systems. Surgical procedure is carried out by a separate mechanism which is attached to the end of the robot and conventional robot is used to positioning this mechanism. These mechanisms are called Remote Center of Motion (RCM) mechanism [1].

The purpose of the RCM mechanism, provide rotating around the incision point to prevent potential damage of the body tissue by the robot. Instruments enter through this incision point into the body with mechanical control and the robot works.

For reasons such as robots in the operation field covering many places, the difficulty of controlling and maintenance the robot, focuses on fixing the RCM mechanisms to working area and direct drive. For this purpose, two different mechanisms profile as a parallel and spherical are developed. In addition, the spherical mechanisms are designed in two different profiles as serial and parallel. In the aforementioned method, mechanism is fixing either end of a robotic arm or directly to the working zone. For this reason, it can be said RCM point's position is fixed. However, although body structure during operation assumed to be constant, as a result of very small movements happen resulting from the organism's liveliness, for precision surgical applications, researchers tend to develop mechanisms as RCM point moving. For this purpose, Hybrid (Serial-Parallel) mechanisms have emerged. In the hybrid mechanisms, working around the RCM point performed by the serial module, shift the RCM point is performed by the parallel module. In this way, requiring very small linear movement and host rotate around incision point such as eye operations, surgical success is increases [1].

2. Literature

Surgical robots designed up to the day are examined. Some of them are given as example.

2.1. Parallel RCM Mechanisms

This kind of RCM mechanisms is usually acted as a basic component of 2 degree of freedom (DOF) or multi-DOF RCM mechanisms because of its simple structure. The most familiar RCM mechanisms in applications are based on a parallelogram structure, which can easily compose 2-DOF RCM mechanisms. Fig. 1a-f shows a basic configuration of parallelogram-based RCM mechanisms. [2].
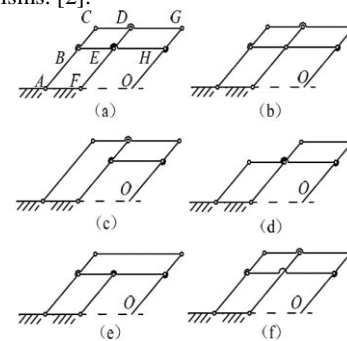

Fig. 1. Parallelogram-based RCM mechanisms [2]

RoboMaster1: In this study, Hadavand at al. studied on a double parallelogram robot called RoboMaster1. A main feature of the double parallelogram mechanism is the fact that the center of rotation is located at a tunable distance from the body of the mechanism. So, this mechanism can be efficiently transferring the remote center of rotation to the back of surgeon's hand without limiting surgeon's maneuvers. For having a stable RCM mechanism, they added another double parallelogram to the mechanism with some offset from the first one as is illustrated in Fig. 2 [3].

---

[1] *Mechatronic Department, Turgut Ozal Univ., Malatya – 44800, TURKEY*
[2] *Mechatronic Eng., Firat University, Elazığ – 23000, TURKEY*
* Corresponding Author: Email: serhat.aksungur@ozal.edu.tr
ORCID Number: 0000-0001-9707-3799

Fig. 2. RoboMaster1 [3]

Development of a Novel Mechanism for Minimally Invasive Surgery: In this paper, a novel robotic system that can assist minimally invasive surgery is proposed by Wang at al. The system has two subsystems: a 3-DOF arm part and 4-DOF instruments. The arm part has a new remote center-of-motion mechanism, while the 4-dof instruments with the diameter 8mm can increase the dexterity during the surgery. The structure of the double parallelogram is simple, and it can fulfill the requirements of the incision point constraints without extra degree of freedom. So it is adopted in many MIS robot systems as the arm part (Fig. 3) [4].
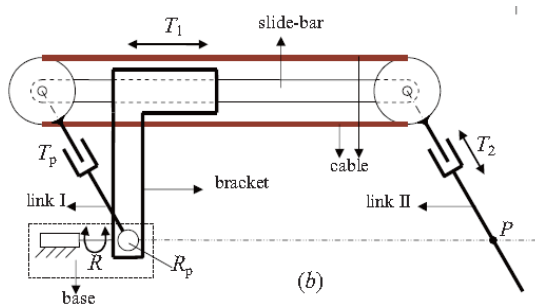

Fig. 3. Mechanism for MIS robot [4]

2.2. Spherical RCM Mechanisms

Promis: Laribi at al. work on developing a compact system for robot-assisted surgery. A PROMIS (Prime RObot for Minimally Invasive Surgery) system is designed for collaborative operation between the surgeon and the robot. The mechanism under study is member of a class of spherical mechanism in which all the links rotation axes intersect at a single point located at the center of the mechanism which shown in Fig. 4. The pivot point makes the spherical mechanism a natural candidate [5].
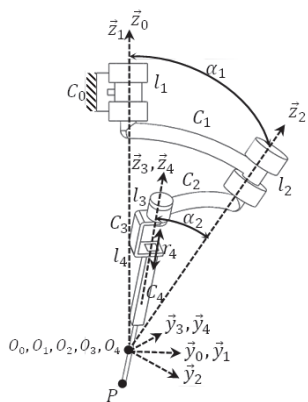

Fig. 4. PROMIS RCM mechanism [5]

Curved RCM Arm: Disclosed is a linkage structure for a surgical robot arm. The first, second and third axes being formed such that extended lines of the three axes are concentrated on a predetermined point of a fore-end of the instrument. An active

type RCM of robot arm according to the present invention allows a fore-end of an instrument to freely pivot around an incision point of the instrument without injuring tissues and to perform precise spherical motion (Fig. 5) [6].
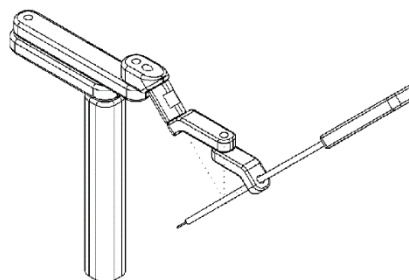
Fig. 5. Curved RCM robot arm [6]

The Spherical Laparoscope Holding Robot: The spherical parallel laparoscope holding robot shown in 4. Its most special feature is that all three branches move on the surface of a virtual sphere. In other words, the rotation center is located at the incision point, where all of the rotational axes coincide. When the incision point is matched to the center of the virtual sphere, the laparoscope could rotate about that point without damaging the incision hole (Fig. 6) [7].
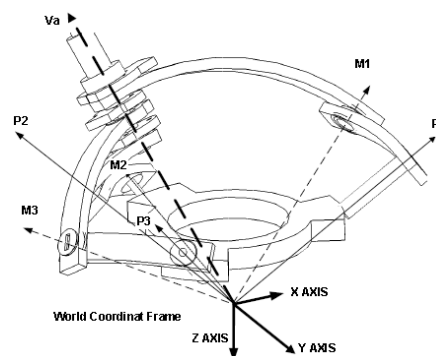
Fig. 6. The schematics drawing of the spherical robot platform [7]

Accurate Linked Mechanism: Yousef and Aiash studied on designed a compact mechanism to enable manipulation about a pivot point, different kinds of surgical tools which are commonly used in minimally invasive surgery such as therapy laser delivery tools, biopsy and bracytherapy needles. The robot comprises two arcuate links as shown in Fig. 7 and a sliding block that is used as a tool adapter. The tool is inserted to pass through the sliding block. Each arcuate link consists of double-curved guidance rods parallel to each other [8].
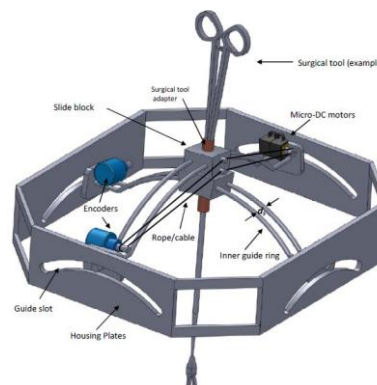
Fig. 7. The proposed robot with a surgical tool [8]

2.3. Hybrid RCM Mechanisms

Eye Robot 2 (ER2): In this study, Üneri at al. present the design of a new generation, cooperatively controlled microsurgery robot with a (RCM) mechanism and an integrated

custom micro-force sensing surgical hook (Fig. 8). A parallel six-bar mechanism has implemented that mechanically provides the isocentric motion, which minimizes the translation of XYZ stages. The resulting robot manipulator consists of four subassemblies. XYZ linear stages for translation;

    b) a rotary stage for rolling

    c) a tilting mechanism with a mechanical RCM and

    d) a tool adaptor with a handle force sensor. [9]

Fig. 8. ER2 robot and close up view of its end effector [9]

None of the mechanisms mentioned in the literature except the hybrid mechanisms, the RCM point cannot set. Especially the structure of parallel mechanisms does not allow this. In hybrid mechanisms, the working parallel mechanism is positioned via a serial manipulator, so that the RCM point can be shifted. This 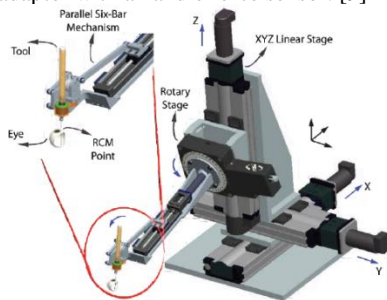increases the number of degrees of freedom of the mechanism and therefore the number of motors and limbs that need to be controlled.

3. Designed Surgical Robot

Literature of robots used for surgical purposes has been scanned and an original surgical robot which is not in literature has been designed.

Robots to be used in surgical operations must be fixed. The patient also needs to be fixed to ensure that the required center of rotation is not moving. In this study, the mechanism has 4 degrees of freedom and the RCM point is designed to be controlled vertically downwards, and the patient's obligation to fix has been abolished. All parts of the designed robot were created with 3 dimensional design program, solid model assembly of the robot was obtained and animations were realized. The designed manipulator has an original design capable of both serial and parallel motion. It is aimed at achieving a wider working volume at depth by performing the movements vertically downward. In the design phase, it is aimed to expressing both kinematic and dynamic equations in a simple way, and providing convenience in mathematical operation. Mathematical expressions of a mechanism with circular joint are more complex and controllability of the circular mechanisms is more difficult than mechanisms in which have linear joints. Therefore, linear joints are predominantly preferred in the designed system.

With this design, the system will not be mounted on the operating table but will be positioned in the upper areas of the table, and then the operational maneuver area of the health personnel and the operator working during the operation will be expanded and the operational capability will be increased.

Mounting state of the designed robot is shown below. Depending on the robot's limbs and the strokes of the linear motors to be used, the working space of the robot has been observed in a 3D environment.

The symbolic design of the mechanism is shown in Fig. 9.
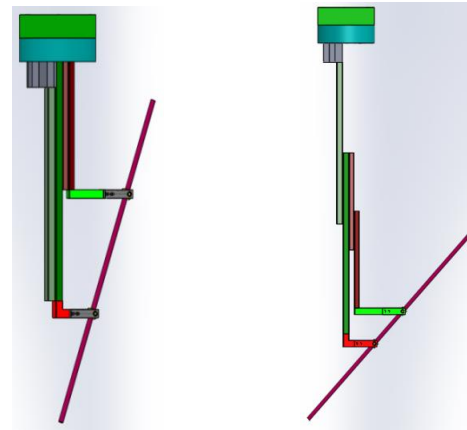
Fig. 9. Design of the mechanism
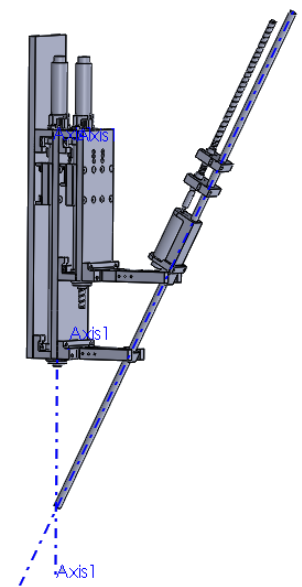
Fig. 10. 3D design of the mechanism

Fig. 9 shows the front view of the mechanism, and Fig. 10 shows the 3D design of the mechanism.

The upper holder is mounted on linear motor No. 3, the lower holder is mounted on linear motor No. 1. The cannula passes through the cannula bearings which are mounted in these holders. The vertical movement of the linear motors 1 and 3 changes the "ϕ" which is the cannula angle. Linear motor number 3 is mounted on linear motor number 1. The placement of this component is shown in Fig. 11.

Fig. 11. Placement of linear motors and cannula holders

The aim of the designed mechanism is to change the angle made by horizontal rotation of the cannula passing through this point without losing the center of rotation point, which is defined as RCM point, and also to rotate the cannula around this point.

The variables used when moving cannula are the cannula angle "ϕ", the rotation of the robot about Z axis "q2", the displacements of the motors that move the holders vertically "q1" and "q3" and the amount of cannula advance "q4". These variables are shown in Fig. 12.

Fig. 12. Schematic representation of the mechanism

4. Kinematic and Dynamic Equations of the Robot

The positions of the 4 points specified on the robot are as follows which are shown in **Hata! Başvuru kaynağı bulunamadı.**.

$$
\begin{aligned}
&A\left(0, 0, \left(q_1 + q_3 + b\right)\right) \\
&B\left((a+c)\cos q_2, (a+c)\sin q_2, \left(q_1 + q_3\right)\right) \\
&C\left(d\cos q_2, d\sin q_2, q_1\right) \\
&D\left(0, 0, q_1\right)
\end{aligned}
\tag{1}
$$

The position equations of the robot end point P (x, y, z) are given below.

$$
\begin{aligned}
P_x &= \left[d - q_4 \cos(\phi)\right]\cos(q_2) \\
P_y &= \left[d - q_4 \cos(\phi)\right]\sin(q_2) \\
P_z &= q_1 - q_4 \sin(\phi)
\end{aligned}
\tag{2}
$$

The Energy equations of the robot are as follows.

Potential energy of the robot;

$$
\begin{aligned}
V &= m_1 \cdot g \cdot q_1 + m_2 \cdot g \cdot \left(q_1 + q_3\right) \\
&+ m_3 \cdot g \cdot \left(q_1 - q_4 \cdot \sin(\phi)\right)
\end{aligned}
\tag{3}
$$

Kinetic Energy of the robot;

$$
\begin{aligned}
T &= \frac{1}{2}\cdot m_1 \cdot \dot{q}_1^{\,2} + \frac{1}{2}\cdot I_{m_1}\cdot \dot{q}_2^{\,2} \\
&+ \frac{1}{2}\cdot m_2 \cdot \left(\dot{q}_1 + \dot{q}_3\right)^2 + \frac{1}{2}\cdot I_{m_2}\cdot \dot{q}_2^{\,2} \\
&+ \frac{1}{2}\cdot m_3 \cdot \left(\dot{X}^2 + \dot{Y}^2 + \dot{Z}^2\right)
\end{aligned}
\tag{4}
$$

Lagrangian equation is

$$
L = T - V
\tag{5}
$$

Euler-Lagrange differential equation is

$$
\frac{d}{dt}\left(\frac{\partial L}{\partial \dot{q}_i}\right) - \frac{\partial L}{\partial q_i} = F_i
\tag{6}
$$

The motion equations obtained after the solution with Euler Lagrange function are as follows.

1. Motion equation is

$$
\begin{aligned}
&\left(m_1 + m_2 + m_3\right)\ddot{q}_1 + \left(m_2 - m_3 q_4 \psi \cos\phi\right)\ddot{q}_3 \\
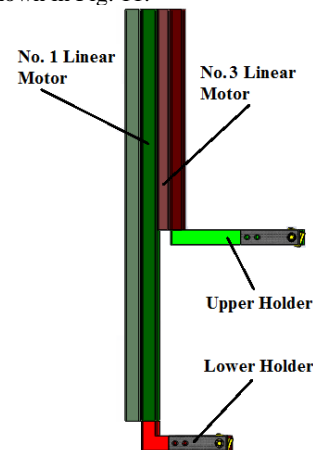&- 2m_3 q_4 \dot{\phi}\cos\phi - m_3 q_4 \dot{q}_3 \dot{\phi}\cos\phi + m_3 q_4 \dot{\phi}^2 \sin\phi \\
&+ \left(m_1 + m_2 + m_3\right)g = F_1
\end{aligned}
\tag{7}
$$

2. Motion equation is

$$
\begin{aligned}
&J_m \ddot{q}_2 + m_3 \ddot{q}_2\left(d^2 + q_4^2 \cos^2\phi - 2d q_4 \cos\phi\right) \\
&+ m_3 \dot{q}_2 2 q_4 \dot{q}_4 \cos^2\phi - 2m_3 \dot{q}_2 q_4^2 \dot{\phi}\cos\phi\sin\phi \\
&- 2m_3 \dot{q}_2 d\dot{q}_4 \cos\phi + 2m_3 \dot{q}_2 q_4 \dot{\phi}\sin\phi = \tau_2
\end{aligned}
\tag{8}
$$

3. Motion equation is

$$
\begin{aligned}
&\left(m_2 + m_3 q_4^2 \psi^2\right)\ddot{q}_3 + \left(m_2 - m_3 q_4 \psi \cos\phi\right)\ddot{q}_1 \\
&+ m_3 q_4 \begin{pmatrix} 2\dot{q}_4 \dot{\phi}\psi + q_4 \psi \dot{q}_3 \dot{\psi} + q_4 \dot{\phi}\dot{\psi} - \dot{q}_1 \dot{\psi}\cos\phi \\ + \dot{q}_1 \psi \dot{\phi}\sin\phi \end{pmatrix} \\
&- m_3 \dot{q}_1 \dot{q}_4 \psi \cos\phi \\
&- m_3 \begin{bmatrix} -\dot{q}_2^2 \dot{q}_4^2 \psi \cos\phi\sin\phi + \dot{q}_2^2 d q_4 \psi \sin\phi \\ + \dot{\phi}q_4^2 \dot{\psi} - \dot{q}_1 \dot{q}_4 \psi \cos\phi + \dot{q}_1 q_4 \dot{\phi}\psi \sin\phi \\ + q_4 g \psi \cos\phi \end{bmatrix} \\
&+ m_2 g = F_3
\end{aligned}
\tag{9}
$$

4. Motion equation is

$$
\begin{aligned}
&m_3 \ddot{q}_4 - m_3 \ddot{q}_1 \sin\phi - m_3 \dot{q}_1 \dot{\phi}\cos\phi \\
&- \dot{q}_2^2\left(m_3 q_4 \cos^2\phi - m_3 d\cos\phi\right) \\
&- m_3 q_4 \dot{\phi}^2 + m_3 \dot{q}_1 \dot{\phi}\cos\phi - m_3 g\sin\phi = F_4
\end{aligned}
\tag{10}
$$

Abbreviations in equations

$$
\phi = a\tan\left(\frac{q_3}{w}\right) \qquad \dot{\phi} = \frac{\dot{q}_3}{w + \dfrac{q_3^2}{w}}
$$

$$
w = a + c - d
$$

$$
\psi = \frac{1}{w + \dfrac{q_3^2}{w}} \qquad \ddot{\phi} = \frac{\ddot{q}_3}{w + \dfrac{q_3^2}{w}} - \frac{2\dot{q}_3^2 q_3}{w^3\left(1 + \dfrac{q_3^2}{w}\right)^2}
$$

$$
\dot{\psi} = \frac{2\dot{q}_3 q_3}{w^3\left(1 + \dfrac{q_3^2}{w}\right)^2} \qquad \ddot{\phi} = \ddot{q}_3 \psi + \dot{q}_3 \dot{\psi}
$$

$$
\tag{11}
$$

5. Fuzzy Control of Robot

Fuzzy control provides a formal methodology for representing, manipulating, and implementing a human's heuristic knowledge about how to control a system.

Fuzzy systems have been used in a wide variety of applications in engineering, science, business, medicine, psychology, and other fields. For instance, in engineering some potential application areas are Aircraft/spacecraft, Automated highway systems, Automobiles, Autonomous vehicles, Manufacturing systems, Power industry, Process control, Robotics, etc.

The fuzzy controller block diagram is given in Fig. 13, where shown a fuzzy controller embedded in a closed-loop control system. The plant outputs are denoted by y(t), its inputs are

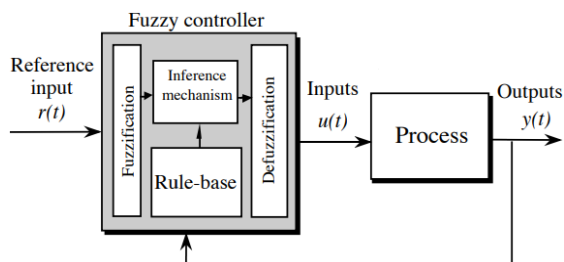denoted by u(t), and the reference input to the fuzzy controller is denoted by r(t).

Fig. 13. Fuzzy controller architecture

The fuzzy controller has four main components: (1) The "rule-base" holds the knowledge, in the form of a set of rules, of how best to control the system. (2) The inference mechanism evaluates which control rules are relevant at the current time and then decides what the input to the plant should be. (3) The fuzzification interface simply modifies the inputs so that they can be interpreted and compared to the rules in the rule-base. And (4) the defuzzification interface converts the conclusions reached by the inference mechanism into the inputs to the plant.

Basically, you should view the fuzzy controller as an artificial decision maker that operates in a closed-loop system in real time. It gathers plant output data y(t), compares it to the reference input r(t), and then decides what the plant input u(t) should be to ensure that the performance objectives will be met [10, 11].

MATLAB program was used for robot control. After the Fuzzy control algorithm is written, the differential equation is solved by the RUNGE KUTTA method. The obtained fuzzy parameters are optimized by genetic algorithm method. For each variable (q1, q2, q3 and q4) a membership function is defined. The fuzzy parameters of each membership functions are given in Table 1.

Table 1. Membership function parameters for each input variable

	P1	P2	P3	P4	P5	P6
q1	-2142,2	-496	-11,8	1,8	6,6	1895,6
q2	-886,6	-328,5	-2,8	2,4	42,4	1988,2
q3	-593,6	-100,2	-16,3	0,5	15,6	1020,5
q4	-449,2	-181,7	-0,5	3,91	8,13	287,7

The graphic of fuzzy logic control input membership functions is shown in Fig. 14.
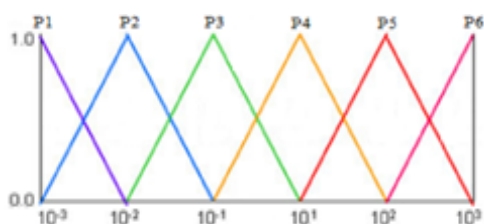

Fig. 14. Input Membership functions

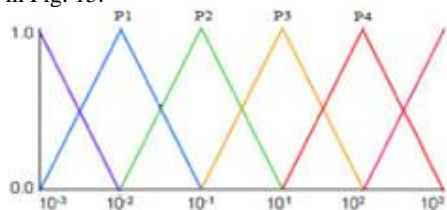The graphic of fuzzy logic control output membership functions is shown in Fig. 15.

Fig. 15. Output membership function

In the MATLAB simulation, the reference values of control are given in Table 2.

Table 2. References of each variable

	References	Motion
q1	0 – 0,1 meter (100 mm)	Linear motion of motor 1
q2	0 – 30° degrees	Rotation of motor 2
q3	0 – 0,1 meter (100 mm)	Linear motion of motor 3
q4	0 – 0,1 meter (100 mm)	Linear motion of motor 4 (cannula)

Position-settling time graphics for each motor is shown in Fig. 16. As can be seen from the graphs, the longest settling time is about 0.7 seconds.
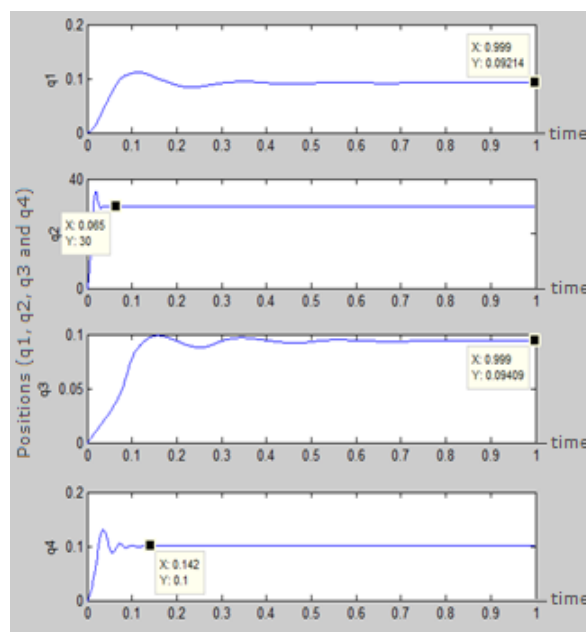

Fig. 16. Position - Settling time graphics for each motor

The graphs of the control signals (u_i) for the system are shown in Fig. 17. As can be seen from the graphics, the longest settling time is about 0.3 seconds.
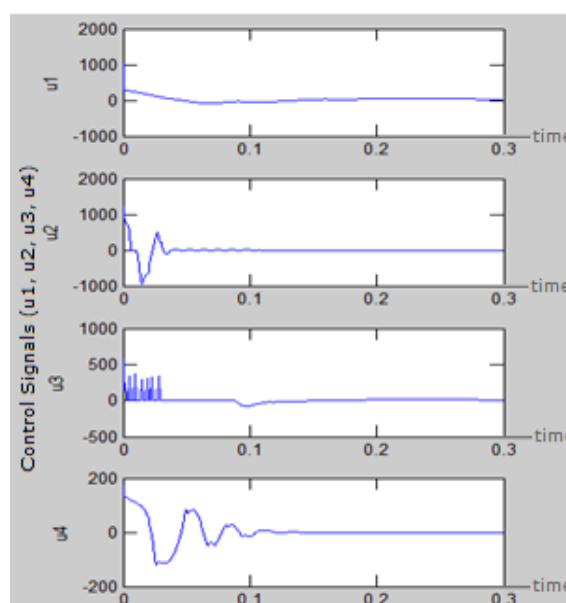

Fig. 17. Control signals – Settling time graphics for each motor

6. Conclusion

In this study, it has been mentioned a robot which is designed to be used in laparoscopic surgery. The most important feature of the robot is that the motions are realized as vertical as possible and the dynamic loads are reduced. The design was mostly created using linear joints. The only rotary joint used to provides the rotation of the robot. That is, the rotation of the point P (x, y, z) depends to only the rotary motor. Thus the motion equations of the robot are obtained in a very simple way [1].

The purpose of the robot is to turn and orient the cannula around the RCM point. It is also possible that the RCM point can be adjusted instantaneously in the vertical axis with the realized design. This will be especially effective in minimizing any mistakes that can occur during a surgical operation. The robot does not occupy space in the field of operation thanks to its structure, so there is more working area for the operation staff.

As the position graphs were examined, it was seen that the robot has arrived to the determined position as soon as possible. The average settling time is 0.4 seconds and the longest settling time is about 0.7 seconds. The error between the desired position and the reached position is due to the gaps in the mechanical connections used at the joint of the robot. The results of position control values are summarized in Table 3.

Table 3. Location errors and settlement times for each position variable

Variable	Desired Position	Reached Position	Position Error	Settling Time (s)
q1 (meter)	0.1	0.092	0.008	~ 0.7
q2 (degree)	30°	30°	0.0	~ 0.06
q3 (meter)	0.1	0.094	0.006	~ 0.7
q4 (meter)	0.1	0.1	0.0	~ 0.014

In the control signal (u_i) graphics, it is seen that approximately 0.3 seconds later all torque values are set. At the end of 0.3 second, torque values are shown as about 32 N for motor 1, 0.1 N for motor 2, 9.5 N for motor 3, and 1 N for motor 4. The results of torque values which are the results of control signal are given in Table 4.

Table 4. Torque values and settlement times for each control variable

Variable	Torque Value (N)	Settling Time (s)
u1	32	~ 0.3
u2	0.1	~ 0.1
u3	9.5	~ 0.27
u4	1	~ 0.15

References

[1] S. Aksungur and T. Koca, "Remote Center of Motion (RCM) Mechanisms for Surgical Operations", International Journal of Applied Mathematics, Electronics and Computers, Vol. 3, No. 2, pp. 119-126, 2015

[2] P. Xu, Y. Jingjun, and B. S. Z. Guanghua, "Enumeration and Type Synthesis of One-DOF Remote-Center-of-Motion Mechanisms," in 12th IFToMM World Congress, , 2007, p.1-6.

[3] M. Hadavand, A. Mirbagheri, H. Salarieh, and F. Farahmand, "Design of a Force-Reflective Master Robot for Haptic Telesurgery Applications: RoboMaster1" in 33rd Annual International Conference, 2011, p. 7037-7040.

[4] J. Li, S. Wang, X. Wang, C. He, and L. Zhang, "Development of a Novel Mechanism for Minimally Invasive Surgery", in International Conference on Robotics and Biomimetics, 2010, p. 1370-1375.

[5] M. A. Laribi, T. Riviere, M. Arsicault, and S. Zeghloul, "A design of slave surgical robot based on motion capture" in International Conference on Robotics and Biomimetics, 2012, p. 600-605.

[6] J. S. Won, S. W. Choi, and W. Peine, "Curved RCM of Surgical Robot Arm", Patent WO 2009/104853 A1, Aug. 27,2009.

[7] J. K. Hsu, T. Li, and S. Payandeh, "On Integration of a Novel Minimally Invasive Surgery Robotic System", IEEE, 2005, p. 437-444.

[8] B. F. Yousef, and F. M. T. Aiash, "A Mechanism for Surgical Tool Manipulation", IEEE, 2013.

[9] A. Üneri, M. A. Balicki, J. Handa, P. Gehlbach, R. H. Taylor, and I. Iordachita, "New Steady-Hand Eye Robot with Micro-Force Sensing for Vitreoretinal Surgery", in 3rd IEEE RAS & EMBS International Conference on Biomedical Robotics and Biomechatronics, 2010, p.814-819.

[10] K. M. Passino and S. Yurkovich, Fuzzy Control, 1st ed., California, USA: Addison Wesley Longman, 1997.

[11] H. T. Nguyen, N. R. Prasad, C. L. Walker and E. A. Walker, A First course in Fuzzy and Neural Control, 1st ed., NY, USA: Chapman & Hall/CRC, 2002.